ICAS 2021 SHANG HAI
International Council of the Aeronautical Sciences
32nd Congress of the International Council of the Aeronautical Sciences
September 6-10, 2021 Pudong Shangri-La, Shanghai, China

STUDY ON ADJOINT OPTIMIZATION OF BWB CONFIGURATION CONSIDERING THE INFLUENCE OF INTAKE AND EXHAUST SYSTEM

Huang Jiangtao[1], Zhou Zhu[1], Gao Zhenghong[2], Chen Xian[1] & Zhong Shidong[1]

[1]China Aerodynamics Research and Development Center, MianYang, Sichuan
[2]Northwestern Polytechnical University, Xi'an, Shan xi

Abstract

For the integrated design of internal and external flow of aircraft, the intake and exhaust boundary conditions of discrete adjoint equation under the power state of propulsion system are studied. The chain derivation rule is used to avoid direct variations of conservative variables. The difficulty of variations of intake and exhaust boundary conditions is greatly simplified by introducing intermediate variables, then the efficient sensitivity analysis method for design variables of exhaust effect is presented. The accuracy of numerical simulation of intake and exhaust is verified by TPS standard model calculation, and the accuracy of adjoint-based sensitivity calculation is verified by comparing with finite difference method. Taking the numerical simulation of intake and exhaust effects of BWB (Blend Wing Body) configuration as an example, the integrated optimization design with or without power conditions was carried out, and the flow field characteristics such as design history, load distribution and pressure distribution under the two conditions were compared and analyzed.

Keywords: Adjoint equation, boundary condition variations, intake and exhaust systems, design variable sensitivity, integrated design

1. Introduction

Aerodynamic configuration/propulsion system integrated design of aircraft has attracted much attention of designers. With the development of high-performance computing and CFD technology, integrated design has become possible. Aerodynamic integrated design of aircraft considering effect of propulsion system is a typical problem in this field. Especially for the configuration of the top-mounted inlet configuration, the effect of intake and exhaust of propulsion system is more obvious [1], which will have an important impact on the sensitivity of design variables. Aerodynamic optimization of aircraft based on discrete adjoint equations has been widely studied [2-7], but most of the adjoint optimization work does not consider the influence of intake and exhaust. An efficient method for calculating the sensitivity of design variables takes into account the influence of intake and exhaust systems is very important for the integrated optimization of aerodynamic configuration. It can provide very effective technical support for aerodynamic configuration integrated design and has important engineering application value.

Based on the large-scale parallel RANS solver independently developed by the research group, the Jacobi derivation of propulsion system boundary conditions is carried out, and an efficient sensitivity analysis method considering the intake and exhaust effects is established, which can provide technical support for the integrated design and analysis of the aerodynamic shape / intake and exhaust system of the aircraft.

2. Gradient solving method based on adjoint equation

For the minimization problem in aerodynamic design:

$$\min_{\text{w.r.t. } D} I(\boldsymbol{W}, \boldsymbol{X}) \tag{1}$$

The residual constraint of flow field is considered as $\boldsymbol{R}(\boldsymbol{W}, \boldsymbol{X}) = 0$. Lagrange operator $\boldsymbol{\Lambda}$ is introduced to construct the following objective function：

$$L = I + \boldsymbol{\Lambda}^T \boldsymbol{R} \tag{2}$$

Among them, the minimum objective function I can be pressure ratio, flow rate, aerodynamic force or other parameters, W, X are the flow field state variables and design variables, further derivation of (2) can get the following expression [8,9]

$$\begin{aligned}\frac{dI}{d\boldsymbol{X}} &= \frac{d}{d\boldsymbol{X}}\left(I(\boldsymbol{W},\boldsymbol{X})+\boldsymbol{\Lambda}^{\mathrm{T}}\boldsymbol{R}(\boldsymbol{W},\boldsymbol{X})\right)\\ &=\left\{\frac{\partial I}{\partial \boldsymbol{W}}\frac{d\boldsymbol{W}}{d\boldsymbol{X}}+\frac{\partial I}{\partial \boldsymbol{X}}\right\}+\boldsymbol{\Lambda}^{\mathrm{T}}\left\{\frac{\partial \boldsymbol{R}}{\partial \boldsymbol{W}}\frac{d\boldsymbol{W}}{d\boldsymbol{X}}+\frac{\partial \boldsymbol{R}}{\partial \boldsymbol{X}}\right\}\\ &=\left\{\frac{\partial I}{\partial \boldsymbol{W}}+\boldsymbol{\Lambda}^{\mathrm{T}}\frac{\partial \boldsymbol{R}}{\partial \boldsymbol{W}}\right\}\frac{d\boldsymbol{W}}{d\boldsymbol{X}}+\left\{\frac{\partial I}{\partial \boldsymbol{X}}+\boldsymbol{\Lambda}^{\mathrm{T}}\frac{\partial \boldsymbol{R}}{\partial \boldsymbol{X}}\right\}\end{aligned} \tag{3}$$

It can be seen from formula (3) that if a suitable operator $\boldsymbol{\Lambda}$ is found so that the first term at the right side equal to aero, the calculation of the $\frac{d\boldsymbol{W}}{d\boldsymbol{X}}$ can be completely eliminated, which is the derivative of flow field state variable w to design variable x, and the expression (4) is obtained

$$\frac{\partial I}{\partial \boldsymbol{W}}+\boldsymbol{\Lambda}^{\mathrm{T}}\frac{\partial \boldsymbol{R}}{\partial \boldsymbol{W}}=0 \tag{4}$$

Formula (4) is the adjoint equation, which can be solved by classical iterative methods such as Jacobi iteration and implicit propulsion, and the sensitivity information can be quickly solved by formula (5).

$$\frac{dI}{d\boldsymbol{X}} = \left\{\frac{\partial I}{\partial \boldsymbol{X}}+\boldsymbol{\Lambda}^{\mathrm{T}}\frac{\partial \boldsymbol{R}}{\partial \boldsymbol{X}}\right\} \tag{5}$$

The right term of formula (5) can be approximately solved by finite difference method:

$$\begin{aligned}\frac{\partial I}{\partial \boldsymbol{X}} &\approx \frac{I(\boldsymbol{W},\boldsymbol{X}+\Delta\boldsymbol{X})-I(\boldsymbol{W},\boldsymbol{X})}{\Delta\boldsymbol{X}}\\ \frac{\partial \boldsymbol{R}}{\partial \boldsymbol{X}} &\approx \frac{\boldsymbol{R}(\boldsymbol{W},\boldsymbol{X}+\Delta\boldsymbol{X})-\boldsymbol{R}(\boldsymbol{W},\boldsymbol{X})}{\Delta\boldsymbol{X}}\end{aligned} \tag{6}$$

In the construction of adjoint equations, the inviscid flux adopts JST scheme, the viscous flux variational adopts thin layer approximation [10], the turbulence model adopts $k-\omega$ SST (shear stress transport) two equation model [11], and the discrete adjoint master equation can be obtained by adding pseudo time term:

$$\begin{aligned}&\boldsymbol{R}_c(\boldsymbol{\lambda})-\boldsymbol{R}_D(\boldsymbol{\lambda})-\boldsymbol{R}_v(\boldsymbol{\lambda})=0\\ &V\frac{\partial \boldsymbol{\lambda}}{\partial t}+\boldsymbol{R}_c(\boldsymbol{\lambda})-\boldsymbol{R}_D(\boldsymbol{\lambda})-\boldsymbol{R}_v(\boldsymbol{\lambda})=0\end{aligned} \tag{7}$$

Among them, $\boldsymbol{R}_c, \boldsymbol{R}_D, \boldsymbol{R}_v$ are the inviscid, artificial viscosity and physical viscosity fluxes corresponding to the adjoint equations, respectively. V, λ are the grid cell volume and the adjoint variables of the flow field. Because equation (7) is consistent with NS equation in form, LU-SGS [12] method and its maximum eigenvalue splitting method can be used to solve discrete adjoint equations. After solving the adjoint equations of the flow field, the sensitivity calculation is carried out by calling the spatial deformation grid technology. Because the flow field does not need to be iterated at this time, the amount of sensitivity calculation is only the time-consuming of grid deformation. In this paper, we use the parallel IDW (Inverse Distance Weighting) grid deformation technology with high computational efficiency [13,14].

3. Boundary Conditions of Discrete Adjoint Equations and the Gradient Verification

Unlike the external flow, the adjoint equation considering the effect of intake and exhaust must take the variations of the power boundary conditions and the intake boundary condition Jacobi of adjoint equation into consideration.

In this paper, the boundary conditions of adjoint equations are treated by matrix method. According to the different properties of boundary conditions, Jacobi $(\frac{\partial \boldsymbol{F}_c(\bar{\boldsymbol{W}})}{\partial \boldsymbol{W}_J})^{\mathrm{T}}_{IJ}$ needs special treatment [15].

Taking the flux calculation of J element close to the boundary of element I as an example, $\boldsymbol{W}_I$ is the conserved variable of boundary element, and $\boldsymbol{W}_J$ is the conserved variable of virtual mesh corresponding to boundary element.

$$\frac{\partial \boldsymbol{F}_c(\bar{\boldsymbol{W}})}{\partial \boldsymbol{W}_I}=\frac{\partial \boldsymbol{F}_c(\bar{\boldsymbol{W}})}{\partial \bar{\boldsymbol{Q}}}\frac{\partial \bar{\boldsymbol{Q}}}{\partial \boldsymbol{Q}_I}\frac{\partial \boldsymbol{Q}_I}{\partial \boldsymbol{W}_I}=\bar{\boldsymbol{A}}\frac{\partial \bar{\boldsymbol{Q}}}{\partial \boldsymbol{Q}_I}\boldsymbol{M}_I \tag{8}$$

Where $\bar{A}, M_2$ are Jacobi matrix and transformation matrix of original variable to conserved variable respectively. It can be seen from equation (8) that the core of boundary condition treatment is to construct the boundary condition matrix $\frac{\partial \bar{Q}}{\partial Q_I}$：

$$\frac{\partial \bar{Q}}{\partial Q_2} = \frac{1}{2}\frac{\partial (Q_1 + Q_2)}{\partial Q_2} = \frac{1}{2}(M_{\mathrm{BC}} + E) \tag{9}$$

Where E, M_{BC} correspond to identity matrix and boundary condition matrix, respectively. However, it is very difficult to deduce the variation of the conserved variables directly by the boundary condition. In order to reduce the difficulty of manual variation derivation, the method of variation and chain derivation of the original variables is used to simplify the derivation process in this paper:

$$M_{\mathrm{BC}} = (\frac{\partial W_J}{\partial Q_J})(\frac{\partial Q_J}{\partial Q_I})_{\mathrm{bc}}(\frac{\partial Q_I}{\partial W_I}) \tag{10}$$

On the CFD numerical simulation of this paper, the inlet boundary condition of the engine is in the specified back pressure form. After the flow field converges, the inlet flow field of the engine fan maintains the characteristics of subsonic pressure exit, and the Jacobi matrix of the inlet boundary condition can be directly derived:

$$M'_{\mathrm{bc}} = (\frac{\partial Q_j}{\partial Q_i})_{\mathrm{bc\_outflow}} = \begin{bmatrix} 1 & & & & \\ & 1 & & & \\ & & 1 & & \\ & & & 1 & \\ & & & & 0 \end{bmatrix} \tag{11}$$

The velocity extrapolation is adopted for the boundary condition of engine outlet, and the total temperature ratio T_t / T_∞ and the total pressure ratio P_t / P_∞ are specified, T_t、T_∞、P_t、P_∞ represent the total temperature, the incoming flow temperature at the engine outlet and the total pressure, the incoming flow static pressure at the engine outlet, respectively. Different from the fan inlet boundary, the variation of engine outlet boundary condition is more complex. We give the Jacobian matrix of engine outlet boundary condition directly.

The exhaust boundary condition Jacobi of adjoint equation:

$$M'_{bc} = (\frac{\partial Q_j}{\partial Q_i})_{\mathrm{bc\_inflow}} = (\frac{\partial Q_j}{\partial f})_{\mathrm{bc\_inflow}}(\frac{\partial f}{\partial Q_i})_{\mathrm{bc\_inflow}} \tag{12}$$

Here, the $\frac{\partial f}{\partial Q_i}$ consists of the following expressions：

$$(\frac{\partial \rho_j}{\partial f})_{bc\_\mathrm{inf}\,low} = -\frac{P_t}{2T_t(\gamma-1)}(1+\frac{\gamma-1}{2}M_j^2)^{-\frac{\gamma}{\gamma-1}}$$

$$(\frac{\partial u_j}{\partial f})_{bc\_\mathrm{inf}\,low} = S_x F_d \sqrt{\gamma R M_j^2 \frac{p_j}{\rho_j}}$$

$$(\frac{\partial v_j}{\partial f})_{bc\_\mathrm{inf}\,low} = S_y F_d \sqrt{\gamma R M_j^2 \frac{p_j}{\rho_j}}$$

$$(\frac{\partial w_j}{\partial f})_{bc\_\mathrm{inf}\,low} = S_z F_d \sqrt{\gamma R M_j^2 \frac{p_j}{\rho_j}}$$

$$(\frac{\partial p_j}{\partial f})_{bc\_\mathrm{inf}\,low} = -\frac{\gamma P_t}{2}(1+\frac{\gamma-1}{2}M_j^2)^{-\frac{-2\gamma+1}{\gamma-1}}$$

$$(\frac{\partial f}{\partial \rho_i})_{bc\_\mathrm{inf}\,low} = \frac{u_i^2+v_i^2+w_i^2}{\gamma p_i}$$

$$(\frac{\partial f}{\partial u_i})_{bc\_\mathrm{inf}\,low} = \frac{2\rho_i u_i}{\gamma p_i}$$

$$(\frac{\partial f}{\partial v_i})_{bc\_\mathrm{inf}\,low} = \frac{2\rho_i v_i}{\gamma p_i}$$

$$(\frac{\partial f}{\partial w_i})_{bc\_\mathrm{inf}\,low} = \frac{2\rho_i w_i}{\gamma p_i}$$

$$(\frac{\partial f}{\partial p_i})_{bc\_\mathrm{inf}\,low} = -\frac{\rho_i(u_i^2+v_i^2+w_i^2)}{\gamma p_i^2}$$

The detailed derivation process of formula (12) and the meaning of variables can be found in reference [1]. In order to check the reliability of the intake and exhaust calculation in this paper, the "NAL-AERO-02-02" TPS (turbine powered simulator) model was used to compare the numerical simulations with the wind tunnel test data. The model was designed by Japan Institute of aerospace technology [16], as shown in Figure 2, X and y are dimensionless coordinates, and the typical flow conditions were selected for numerical verification.

Figure 1 shows the pressure distribution comparison between TPS simulations and wind tunnel test under typical calculation conditions. It can be seen that the intake and exhaust numerical simulation

method can accurately simulate the flow phenomenon of engine intake and exhaust, and provide reliable numerical simulation results for intake and exhaust numerical simulation. Figure 2 shows the calculation and verification of adjoint sensitivity of a flying wing considering engine dynamic effect. It is showed that the developed gradient calculation based on adjoint equation is more accurate, which can provide technical support for the integrated design considering dynamic effect.

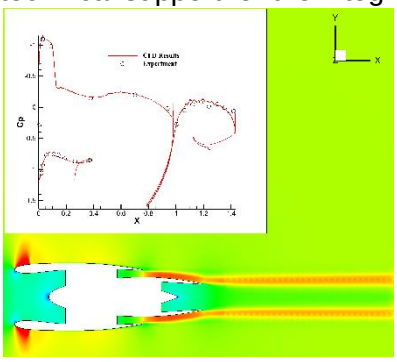

Figure 1 Validation of intake and exhaust calculations

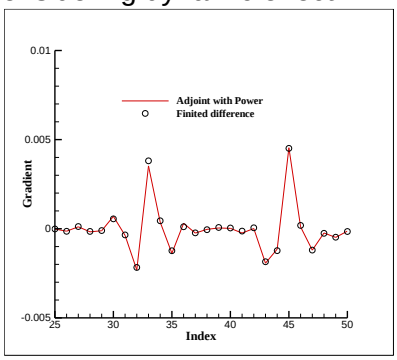

Figure 2 Gradient verification of adjoint equation under intake and exhaust conditions

4. BWB aerodynamic configuration optimization under intake and exhaust conditions

By using the adjoint optimization method established in this paper, the integrated design of BWB configuration for top-mounted inlet configuration is carried out. The design status is as follows：$M=0.85,\ H=11Km,\ CL=0.35$. Figure 3 gives the parameterized sketch of the whole aircraft based on FFD technology, where are 160 design variables. Figure 4 gives the gradient comparison of design variables under different working conditions. It can be seen that the influence of power on the gradient of design variables is obvious. One of the reasons is that the dynamic effect changes the flow pattern on the upper surface, leading to the change of cruise attack angle, which changes the gradient of design variables. Figure 5 and Figure 6 give the optimization process of aerodynamic force and lift-drag ratio with or without power. Figure 7 and Figure 8 give the pressure contour comparison initial and optimal configuration under different condition. Under the condition of high-speed cruise, the power effect makes the front wing of the nacelle appear larger pressure recovery area. Figure 9 to Figure12 show the comparison of the pressure distribution of typical stations before and after optimization. It is showed that the shock wave basically disappears after optimization design, and the biggest difference of pressure distribution between with and or without dynamic effect appears near the nacelle. Although the influence of power decreases with approaching to the wing tip, the difference of pressure distribution of the optimized configuration is obvious in the whole span wise because the power effect changes the cruise angle of attack.

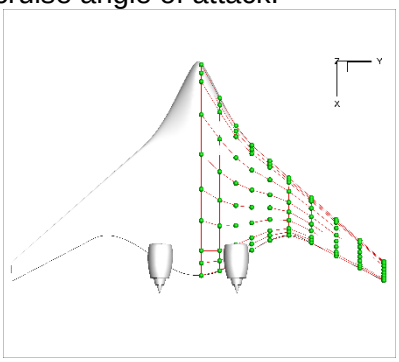

Figure 3 FFD Lattice for BWB configuration

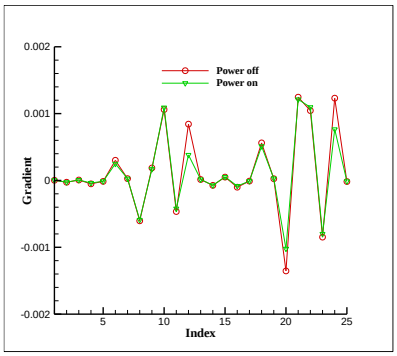

Figure 4 Gradient comparison of different working conditions

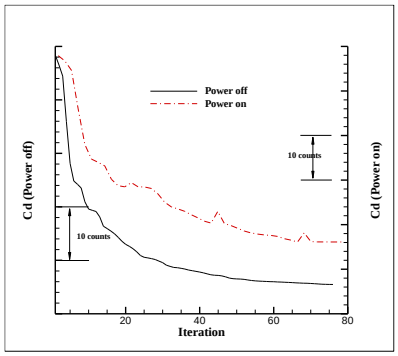

Figure 5 Comparison of drag optimization process under different working conditions

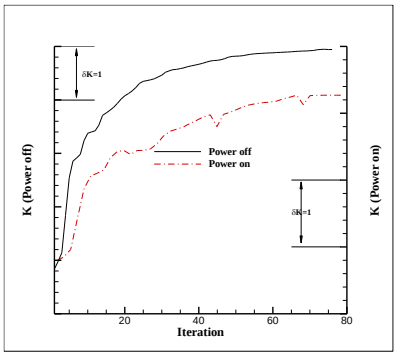

Figure 6 Comparison of lift-drag ratio optimization process under different working conditions

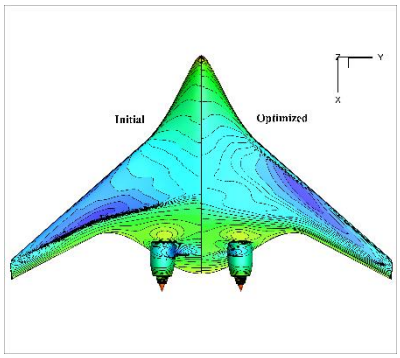

Figure 7 Comparisons of pressure contour of initial and optimal configuration with power

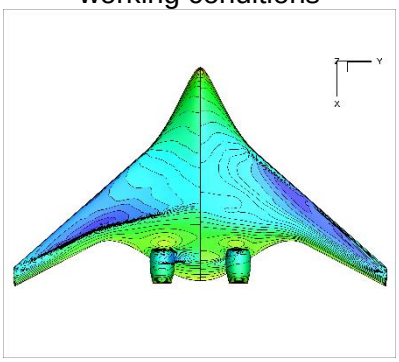

Figure 8 Comparisons of pressure contour of initial and optimal configuration without power

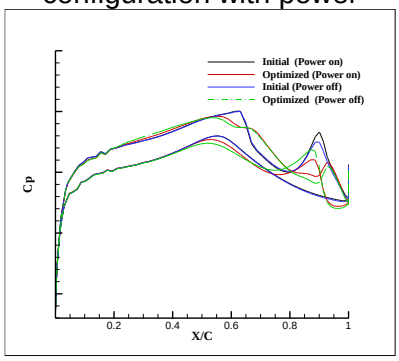

Figure 9 Pressure distribution comparison under different conditions (Y=0)

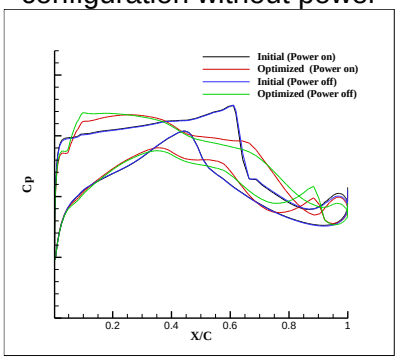

Figure 10 Pressure distribution comparison under different conditions (Y=6)

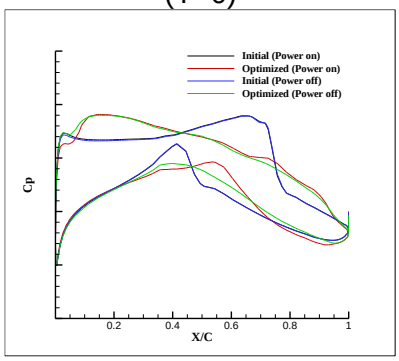

Figure 11 Pressure distribution comparison under different conditions (Y=10)

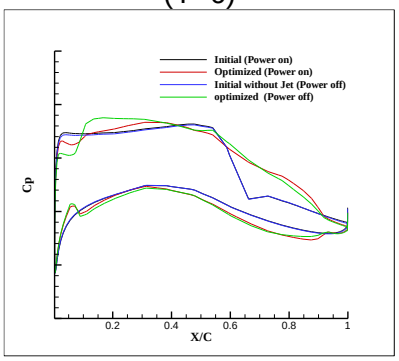

Figure 12 Pressure distribution comparison under different conditions (Y=15)

5. Conclusion

Based on the inlet and exhaust boundary condition Jacobi derivation of discrete adjoint equation, an adjoint optimization system considering propulsion effects is established, and the gradient solution of

adjoint equation is verified. The gradients of design variables under different working conditions are compared, and the results show that the propulsion system has a significant influence on the gradients of design variables. The integrated design of BWB aerodynamic configuration is further carried out. The flow field characteristics such as design history, load distribution and pressure distribution under the two working conditions are compared and analyzed. It shows the necessity of integrated design considering the dynamic effect of propulsion system, and the technology developed in this paper provides strong technical support for aerodynamic design of aircraft with backpack inlet configuration.

6. Contact Author Email Address

Corresponding author: Chen Xian; E-mail: chenxian_lgdx@yeah.net

7. Copyright Statement

References

[1] Huang J-T, Zhou Z and Yu J. Sensitivity Analysis of Design Variables Considering Intake and Exhaust Effects. *JOURNAL OF PROPULSION TECHNOLOGY*, Vol. 40, No. 2, pp 250-258, 2019.
[2] Sobieszczanski-Sobieski J. Sensitivity Analysis and Multidisciplinary optimization for Aircraft Design: Recent Advance and results. *Journal of Aircraft,* Vol. 27, No.12, pp 993-1001, 1990.
[3] Jameson A. Aerodynamic design via control theory. *Journal of Scientific Computing*, Vol. 3, pp233-260, 1988.
[4] Zhou J L and Gaetan K.W. Kenway and Joaquim R. R. A. Martins RANS-based Aerodynamic Shape Optimization Investigations of the Common Research Model Wing. AIAA-20140567.
[5] Amoignon O and Berggren M. Adjoint of a median-dual finite-volume scheme Application to transonic Aerodynamic Shape Optimization. *Technical Report* 2006-3, *Uppsala University,* 2006.
[6] Carpentieri G. An Adjoint-Based Shape-Optimization Method for Aerodynamic Design. *Delft:Technische Universiteit*，2009.
[7] Li B, Deng Y Q, Tang J, et al. Discrete adjoint optimization method for 3D unstructured grid. *Acta Aeronautica et Astronautica Sinica*, Vol. 35, No.3, pp 674-686, 2014.
[8] Dwight R P and Brezillon J. Effect of various approximations of the discrete adjoint on gradient-based optimization. *AIAA-2006-0690*, 2006.
[9] Huang J T, Liu G, Zhou Z, et al. Investigation of gradient computation based on discrete adjoint method. *Acta Aerodynamica Sinica*, Vol. 35, No.4, pp 554-562, 2017.
[10] Blazek J. *Computational Fluid Dynamics: Principles and Applications*. Alstom Power Ltd., Baden-Daettwil, Switzerland, 2001.
[11] Menter F R. Improved two-equation k-ω turbulence models for aerodynamic flows. *NASA TM 103975*, 1992.
[12] Chen R F and Wang Z J. Fast, block lower-upper symmetric gauss-seidel scheme for an artributrary grids. *AIAA Journal*, Vol.1, No.38, pp 2238-22452, 2000.
[13] Luke E, Collins E and Blades E. A fast mesh deformation method using explicit interpolation. *Journal of Computational Physics*, Vol.231, No.2, pp 586-601, 2012.
[14] Uyttersprot L. Inverse Distance Weighting Mesh Deformation a Robust and Efficient Method for Unstructured Meshes. Delft, TU Delft, 2014.
[15] Huang J T, Liu G, Zhou Z, et al. Investigation of gradient computation based on discrete adjoint method. *Acta Aerodynamica Sinica,*Vol.35, No.4, pp 554-562, 2017.
[16] Hirose N, Asai K, and Ikawa K. Trabsonic 3-D Euler analysis of flows around fan-jet engine and TPS (turbine powered simulator). NAL-TR-1045,1989.